Chemical Engineering Science 251 (2022) 117455

Contents lists available at ScienceDirect

Chemical Engineering Science

journal homepage: www.elsevier.com/locate/ces

Towards a general correlation for minimum fluidization velocity in gas-fluidized beds: Based on a database mining from the literature

Jibin Zhou [a], Mao Ye [a,*], Zhongmin Liu [a,b]

[a] National Engineering Laboratory for Methanol to Olefins, Dalian Institute of Chemical Physics, Chinese Academy of Sciences, Dalian 116023, PR China
[b] University of Chinese Academy of Sciences, Beijing 100083, PR China

HIGHLIGHTS

- Empirical correlations were assessed with an established database of U_{mf}.
- The limited applications of empirical correlations were disclosed.
- Four modified formulae of correlations were developed for the prediction of U_{mf}.
- A general correlation of U_{mf} based on direct numerical simulations was proposed.

GRAPHICAL ABSTRACT

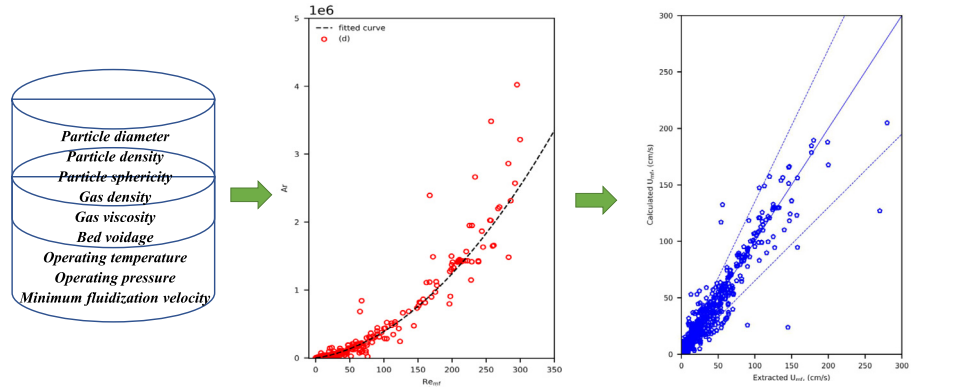

Database mining from literature **Regression analysis** **Performance of the correlation**

ARTICLE INFO

Article history:
Received 30 November 2021
Received in revised form 11 January 2022
Accepted 18 January 2022
Available online 24 January 2022

Keywords:
Minimum fluidization velocity
Gas-fluidized bed
General correlation
Data mining

ABSTRACT

As one of the most significant parameters in fluidized beds design and operation, the minimum fluidization velocity (U_{mf}) has received utmost attention since 1940s. As an effective reference for evaluating the fluidization characteristic, U_{mf} is conventionally predicted using the empirical correlation developed based on experiments for the specified gas-solid system. Despite more than 100 correlations proposed in the literature, these correlations show great diversity in either the applicable regimes or the mathematical formulae. Thus a general correlation for accurately determining U_{mf} is highly desired. In this work, with a recently established database of U_{mf} mined from published papers, the empirical correlations with four different formulae were first assessed for Geldart Groups A, B, and D particles, respectively. In view of the application limitations, modifications to different formulae of empirical correlations have been made to achieve satisfactory performances in predicting U_{mf} for either Geldart Groups A, B, or D particles. Note that U_{mf} is essentially determined by the balance between the gravitational force and drag force for a gas-solid system, a new formula based on a fluidized bed drag correlation derived from direct numerical simulations (DNS) was proposed. By using this formula, we developed a general correlation for U_{mf} in gas-fluidized beds, which exhibits the best performance for all Geldart Groups A, B, and D particles when compared with empirical correlations reported in the literature.

* Corresponding author.
E-mail address: maoye@dicp.ac.cn (M. Ye).

https://doi.org/10.1016/j.ces.2022.117455
0009-2509/

Notation

d	particle diameter (μm)	ρ	density, kg/m^3
U	velocity (cm/s)	ε	minimum fluidization
g	gravitational acceleration (m/s^2)	μ	dynamic viscosity, Pa·s
p	particle	φ	particle sphericity
g	fluidized gas		
mf	minimum fluidization		

1. Introduction

As one of the most important reactors, gas-solid fluidized bed has been widely employed in chemical industrial processes (Liu et al., 2019; Mahmoudi et al., 2010; Sadeghbeigi, 2012; Tian et al., 2015; Wang and Zhu, 2020; Wang et al., 2021) due to its several unique advantages such as the excellent heat and mass transfer capabilities (Gutfinger and Abuaf, 1974). The minimum fluidization velocity (U_{mf}) is considered to be a crucial hydrodynamic parameter for the fluidized beds design and operation, as well as a function of the physical properties of particles and fluidized gases, and operating variables (e.g., temperature and pressure) (Anantharaman et al., 2017; Feng et al., 2017; Sangeetha et al., 2000; Shao et al., 2020; Subramani et al., 2007). However, until now, the relationship between U_{mf} and the functional variables has not been fully explored (Tan et al., 2008). In practice, the accurate prediction of U_{mf} is important for chemical engineers to optimize the performance of the fluidized bed, because U_{mf} sets the lower limit of the gas flow rate required for minimum fluidization (Bilbao et al., 1987). Traditional experimental methods of determining U_{mf} (e.g., pressure drop method (Chiba et al., 1979) and Gaussian spectral pressure distribution (Parise et al., 2008), are time-consuming and also limited to specified conditions. Thus, chemical engineers have been working on developing suitable empirical correlations to predict U_{mf} through methods of dimensional analysis (Coltters and Rivas, 2004; Fang et al., 2020), force balance (Halvorsen and Arvoh, 2009; Xu and Zhu, 2008), and so on. Although these empirical correlations can meet the experimental results satisfactorily within the scope of their development, significant divergences will occur when they are extrapolated to systems with different characteristics from the original system (Fletcher et al., 1992; Gupta et al., 2009). Therefore, a comprehensive qualitative or quantitative assessment of these correlations is necessary. Lots of related works, in fact, have already been carried out. For instance, Fletcher et al. found that some published correlations were not applicable to certain specific Geldart Group B particles and their performances were even worse than the simplified Ergun equation (Fletcher et al., 1992). Gupta et al. also verified that quite a few correlations exhibited large deviations when calculating U_{mf} of some Geldart Group B materials (Gupta et al., 2009). This was also confirmed by Coltters et al., who found that a significant disagreement occurred when the correlations were used to predict U_{mf} in the extractive metallurgical process of ores (Coltters and Rivas, 2004). Recently, Anantharaman et al. conducted a comprehensive and detailed assessment of these empirical correlations available in the published literature for Geldart Groups A, B, and D particles and concluded that almost all correlations had their limitations; they could only exhibit perfect performances in the specific system (Anantharaman et al., 2017). In brief, the empirical nature of the correlations makes it impossible to confidently extrapolate them to systems with different characteristics from the systems they were developed.

In our previous work (Zhou et al., 2021), a database of U_{mf}, containing U_{mf} and other eight functional properties (particle diameter, particle density, particle sphericity, bed voidage, gas density and gas viscosity, operating temperature and pressure) was established by automatic literature data extraction using text mining algorithm. To the best of our knowledge, the database contains the most extensive collection of particle and gas properties, allowing us to make a comprehensive evaluation of these empirical correlations, and more importantly, to develop new correlations with the regression analysis method. Therefore, in this work, the performances of some empirical correlations are first evaluated for Geldart Groups A, B, and D particles with the database, which can give an indication of the range applicability of these correlations. Then, modified correlations are developed by determining the empirical parameters with the database and their performances are also evaluated subsequently. Note that U_{mf} is essentially determined by the balance between the gravitational force and drag force of the gas-solid system, a new formula based on a fluidized bed drag correlation derived from direct numerical simulations (DNS) is proposed. By use of this new formula, a general correlation for determining U_{mf} is developed, which exhibits the best performance for Geldart Groups A, B, and D particles when compared with the modified correlations and empirical correlations reported in the literature.

2. Evaluation criteria

To quantify the differences between the evaluated correlations, some commonly used evaluation criteria are adopted. Firstly, we set the relative error to ±35%, and then calculate the percentage of data points within the relative error range of the total data, which is called predictive capability and abbreviated as *PC*. Besides, the average absolute relative error (*AARE*) and coefficient of determination (R^2) are also calculated, as shown in Eqs.1–2:

$$AARE = \frac{1}{n}\sum_{i=1}^{n}\left|\frac{U_{mf,i}(database) - U_{mf,i}(correaltion)}{U_{mf,i}(database)}\right| \quad (1)$$

$$R^2 = 1 - \frac{\sum_{i=1}^{n}\left(U_{mf,i}(database) - U_{mf,i}(correaltion)\right)^2}{\sum_{i=1}^{n}\left(U_{mf,i}(database) - \overline{U_{mf,i}(database)}\right)^2} \quad (2)$$

where n,$U_{mf,i}(correaltion)$ and $U_{mf,i}(database)$ are the total number of data samples, the calculated value for the ith sample with the specific correlation, and the extracted value for ith sample in the database, respectively. Specifically, the value of one for R^2 indicates that the curve passes through every data point, while the value of zero means the regression model does not describe the data better than a horizontal line passing through the average of the data points. It should be noted that if a correlation is completely inappropriate for predicting U_{mf}, the negative value of R^2 will be given. *AARE* represents the difference between the calculated and extracted values and is used to designate the accuracy of the theoretical models (Hosseini et al., 2019). Therefore, the suitability of a correlation is quantified by higher values of *PC* and R^2, and a lower value of *AARE*.

3. Results and discussions

3.1. Performances of the empirical correlations

Although hundreds of empirical correlations have been proposed since 1940s when the first fluidization work was published, they can be broadly classified into four groups (Anantharaman et al., 2017):

$$Re_{mf} = \mathrm{A} \cdot Ar^{b}$$

$$U_{mf} = K \cdot X^{\alpha} \tag{4}$$

$$Re_{mf} = \frac{Ar}{p + q\sqrt{Ar}} \tag{5}$$

$$Re_{mf} = \left(K_1^2 + K_2 Ar\right)^{0.5} - K_1 \tag{6}$$

herein, A, b, K, α, p, q, K_1, and K_2 are empirical constants, which can be derived by regression analysis based on the experimental data. Ar and Re_{mf} represent the dimensionless Archimedes number and Reynolds number at minimum fluidization, both of which are functions of physical properties of particles and fluidized gases:

$$\mathrm{Ar} = \frac{\rho_g d_p^3 \left(\rho_p - \rho_g\right) g}{\mu^2} \tag{7}$$

$$Re_{mf} = \frac{\rho_g U_{mf} d_p}{\mu} \tag{8}$$

where d_p, ρ_p, ρ_g, μ and g are particle diameter, particle density, gas density, gas viscosity, and gravitational acceleration, respectively.

According to the Geldart classification (Geldart, 1973), the extracted database contains 195, 756, and 265 groups of Geldart Groups A, B, and D particles, respectively (Zhou et al., 2021). Geldart Group C particles are not considered in this work because of the strong inter-particle forces, which makes the fluidization difficult (Geldart, 1973). The specific distribution of each property in the database can be referred to our previous study (Zhou et al., 2021). In the following evaluation work, the influences of operating temperature and pressure are also implicitly reflected on the gas density and viscosity (Shao et al., 2020; Zhou et al., 2021).

3.1.1. Performances of empirical correlations with $Re_{mf} = A \cdot Ar^{b}$ type

Since dozens of such correlations of this type have been proposed, in this work, we selectively evaluated six correlations of them, as listed in Table 1. Note that the correlation of Baeyens et al. (Baeyens and Geldart, 1973) was originally developed for Geldart Group A particles, here, however, we also evaluated it against Geldart Groups B and D particles following the review (Anantharaman et al., 2017). The comparisons between the calculated and extracted values of U_{mf} for all Geldart Groups particles with the boundaries corresponding to ±35% error are shown in Fig. 1. And the individual comparison results for Geldart Group A, B, and D particles are shown in Figs. S1-S3, respectively. Moreover, Table 1 gives the statistical analysis results of these correlations in terms of *AARE*, R^2, and *PC*. U_{mf} for most practical gas-solid systems is within 0–2 m/s, and it is seldom to find U_{mf} larger than 2 m/s. A careful check with the data sets mining from the literature showed that U_{mf} of 2.80 m/s and 2.70 m/s were exceptionally obtained for ceramic ball of 5.6 mm (Jing et al., 2001) and char agglomerates of 5.0 mm (Laugwitz et al., 2017), respectively. Note that in both cases the bed materials are essentially Geldart Group D particles.

It is clearly seen from Fig. 1 that the shapes of the curves for these six selected correlations have striking similarities, and they all over-predict the U_{mf}. Particularly, when the values of extracted U_{mf} are greater than ~70 cm/s, the discrepancy between the calculated and extracted U_{mf} begins to increase significantly, and the calculated values are almost an order of magnitude of the extracted values. Results shown in Figs. S1-S3 indicate that for any Geldart Group particles, the correlation proposed by Tannous et al. (Tannous and Lourenço, 2015) gives the lowest predictive capability and overestimates the U_{mf}, presumably because the mixture of biomass particles was used to measure the U_{mf} and derive the correlation in their work. This result suggests that the correlation derived from mixed particles has certain limitations and may not be suitable for the monodisperse particle system.

As depicted in Table 1, when used as a correlation to determine U_{mf} of Geldart Groups A, B and D particles at the same time, the values of R^2 for these six correlations are all negative. This is especially true for Geldart Group D particles. And this makes it clear that this type of correlation obviously cannot be used as a general correlation for the prediction of U_{mf} of all Geldart Group particles. For Geldart Groups A and B particles, except for the correlation of Tannous et al. (Tannous and Lourenço, 2015), most of the data points are scattered within the given error range, and the lowest values of *PC* are ~62.6% and ~70.5%, respectively. It is also noticed that these correlations are inclined to underestimate U_{mf} for Geldart Groups A and B particles (Figs. S1-S2). The average values of R^2 for Geldart Groups A and B particles are 0.404 and 0.544, respectively. And the average values of *AARE* are both small and around 0.3. These results indicate that, different from the conclusion of Geldart Group D particles, these correlations can be used to predict U_{mf} for Geldart Groups A and B particles to some extent. The huge performance differences among each Geldart Group particles may be due to the fact that these correlations were mainly developed for particles with diameters less than 2000 μm. However, the particle diameter distribution in our extracted database is relatively wide, especially when the U_{mf} is greater than ~70 cm/s, the

Table 1
Statistical analysis results for different correlations with $Re_{mf} = A \cdot Ar^{b}$ type.

Researchers	Correlations	A			B			D			All		
		AARE	R^2	PC	AARE	R^2	PC	AARE	R^2	PC	AARE	R^2	PC
Leva (Leva, 1959)	$Re_{mf} = 0.000822Ar^{0.94}$	0.342	0.322	62.6%	0.309	0.454	70.5%	0.753	−18.17	53.2%	0.411	−5.359	65.5%
Pillai et al. (Pillai and Rao, 1971)	$Re_{mf} = 0.000701Ar$	0.334	0.463	66.2%	0.331	0.602	72.8%	2.036	−129.63	23.0%	0.703	−42.086	60.9%
Baeyens et al. (Baeyens and Geldart, 1973)	$Re_{mf} = 0.0009125Ar^{0.934}$	0.344	0.346	64.6%	0.291	0.487	74.6%	0.772	−18.620	52.1%	0.404	−5.505	68.1%
Doichev et al. (Doichev and Akhmakov, 1979)	$Re_{mf} = 0.00097Ar^{0.947}$	0.371	0.417	64.6%	0.289	0.581	77.1%	1.120	−37.683	39.2%	0.483	−11.781	66.9%
Fletcher et al. (Fletcher et al., 1992)	$Re_{mf} = 0.000714Ar$	0.335	0.471	65.6%	0.342	0.598	72.2%	2.091	−135.153	20.0%	0.722	−43.906	59.8%
Tannous et al. (Tannous and Lourenço, 2015)	$Re_{mf} = 0.0123Ar^{0.8086}$	7.334	−1.937	4.1%	3.757	−7.39	0.7%	3.344	−98.486	0.0%	4.241	−32.414	1.1%

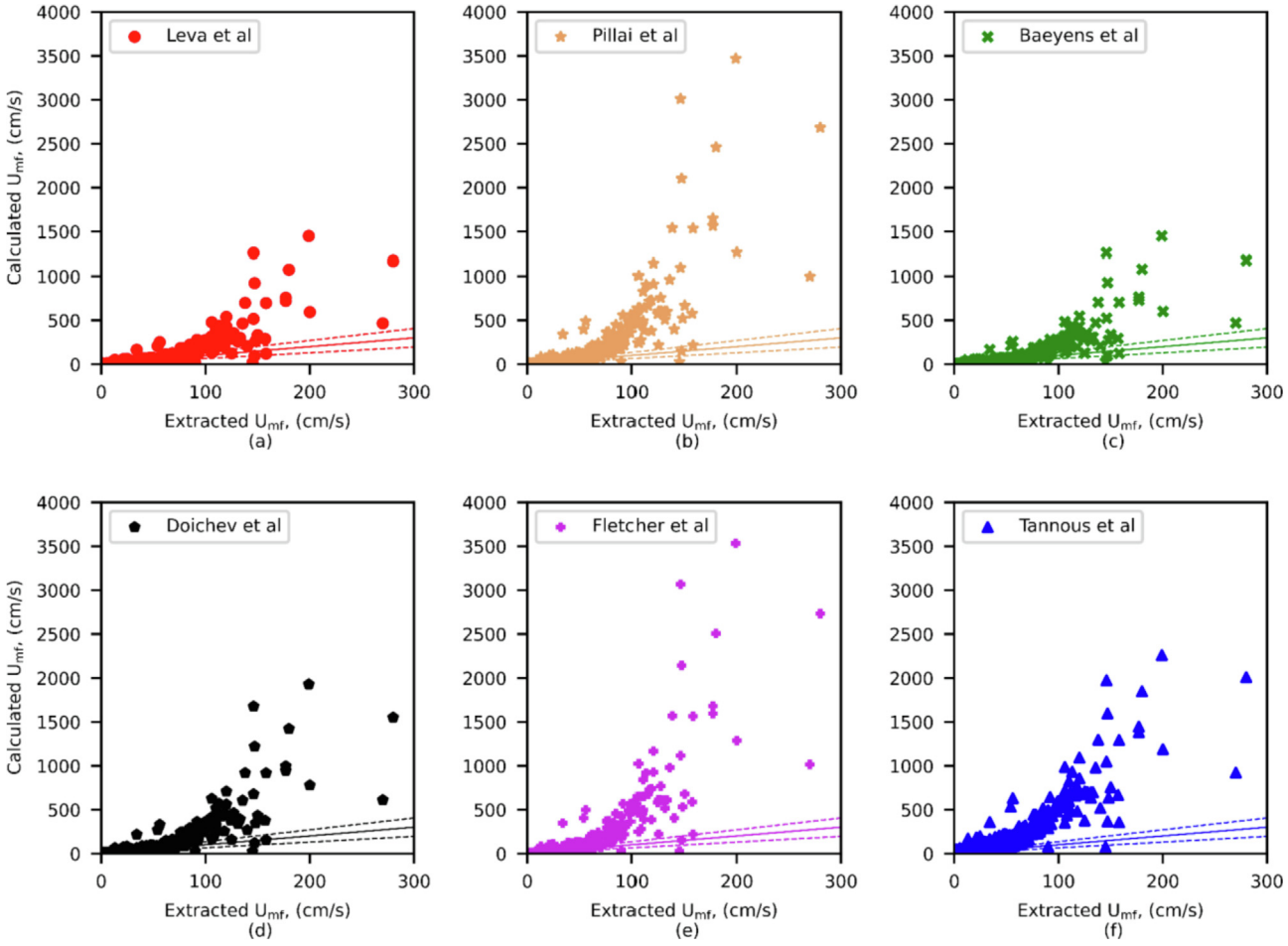

Fig. 1. Comparisons between the values of calculated and extracted U_{mf} for different correlations with $Re_{mf} = A \cdot Ar^b$ type.

corresponding particle diameter is always greater than 2000 μm, which is beyond the scope of their study.

In summary, for this type of correlation, it has certain limitations and cannot be used as a general correlation to simultaneously predict U_{mf} of all Geldart Groups particles. However, as correlations to predict U_{mf} of individual Geldart Group particles, they exhibit different predictive capabilities. Specifically, the correlation of Fletcher et al. (1992) gives the best performance for Geldart Group A particles with the highest values of *PC* (~65.6%) and R^2 (0.471), and the lowest value of *AARE* (0.335). The correlation of Doichev et al. (Doichev and Akhmakov, 1979) gives the best performance for Geldart Group B particles with the highest values of *PC* (~77.1%) and R^2 (0.581), and the lowest value of *AARE* (0.289). And all these correlations are not suitable in prediction of U_{mf} for Geldart Group D particles.

3.1.2. Performances of empirical correlations with $\boldsymbol{U_{mf} = K \cdot X^{\alpha}}$ type

It is well accepted that U_{mf} is sensitive to properties of particles and fluidized gases, hence, Coltters et al. proposed a new type of correlation that only considered the physical properties of particles and fluidized gases using the dimensional analysis method (Coltters and Rivas, 2004).

$$U_{mf} = K \cdot X^{\alpha} \tag{9}$$

$$X = \left(\frac{\left(\rho_p - \rho_g\right) g d_p^2}{\mu_g}\right)\left(\frac{\rho_p}{\rho_g}\right)^{1.23} \tag{10}$$

where X is a function of d_p, ρ_p, ρ_g, μ_g, and g. The empirical constants K and α can be determined by data-fitting with the experimental data.

Similarly, to illustrate the performance of this type of correlation, six correlations (as listed in Table 2) are selected, and the qualitative comparison results are shown in Fig. 2 and Figs. S4-S6. Compared with the results of the first type of correlation shown in Fig. 1, the differences between the values of calculated and extracted U_{mf} for this type are not significant. However, some noteworthy differences are made for these correlations due to the differences in empirical constants. First of all, the performances can be divided into two cases, one is the under-prediction of U_{mf} (Fig. 2a, c, d), and the other is the overestimation of U_{mf} (Fig. 2b, e, f), which is particularly consistent with the results of Geldart Group D particle (Fig. S6). Secondly, it is noticed in Fig. S4 that except for correlations of Coltters et al. (a) and (e) (Coltters and Rivas, 2004), the other four correlations obviously over-predict U_{mf} of Geldart Group A particles. For Geldart Group B particles (Fig. S5), the correlation of Coltters et al. (a) (Coltters and Rivas, 2004) underestimates the U_{mf}, while for the other five correlations, the data points are scattered, with both overestimation and underestimation. These results indicate that the performances of these correlations are very sensitive to the empirical constants.

Examination of Table 2 reveals that compared with the first type of correlation, this format of correlation presents a worse predictive capability for Geldart Groups A and B particles, but gives a better predictive capability for Geldart Group D particles. To be specific, the values of R^2 are all negative for Geldart Group A

Table 2
Statistical analysis results for different correlations with $U_{mf} = K \cdot X^{\alpha}$ type.

Researchers	Correlations	A			B			D			All		
		AARE	R^2	PC	AARE	R^2	PC	AARE	R^2	PC	AARE	R^2	PC
Coltters et al. (a) (Coltters and Rivas, 2004)	$U_{mf} = 4.7673*10^{-6}X^{0.71635}$	0.685	−0.194	33.8%	0.609	−0.279	17.5%	0.632	−0.386	7.5%	0.626	0.447	17.9%
Coltters et al. (b) (Coltters and Rivas, 2004)	$U_{mf} = 1.145*10^{-5}X^{0.71957}$	1.865	−0.744	20.5%	1.050	−0.146	32.8%	0.497	−1.852	49.8%	1.060	−0.027	34.5%
Coltters et al. (c) (Coltters and Rivas, 2004)	$U_{mf} = 7.9265*10^{-4}X^{0.50953}$	4.167	−0.835	3.1%	1.140	0.162	30.8%	0.360	0.409	50.2%	1.455	0.741	30.6%
Coltters et al. (d) (Coltters and Rivas, 2004)	$U_{mf} = 7.1187*10^{-5}X^{0.61787}$	1.727	−0.377	17.4%	0.700	0.129	45.5%	0.406	0.366	44.2%	0.800	0.725	40.7%
Coltters et al. (e) (Coltters and Rivas, 2004)	$U_{mf} = 4.3384*10^{-7}X^{0.89029}$	1.044	−0.512	38.5%	0.776	−0.240	50.1%	0.810	−12.353	39.6%	0.826	−3.494	46.0%
Zhong et al. (Zhong et al., 2008)	$U_{mf} = 1.2*10^{-4}X^{0.633}$	4.498	−2.034	3.1%	2.054	−1.235	14.7%	0.679	−2.868	37.0%	2.146	−0.444	17.7%

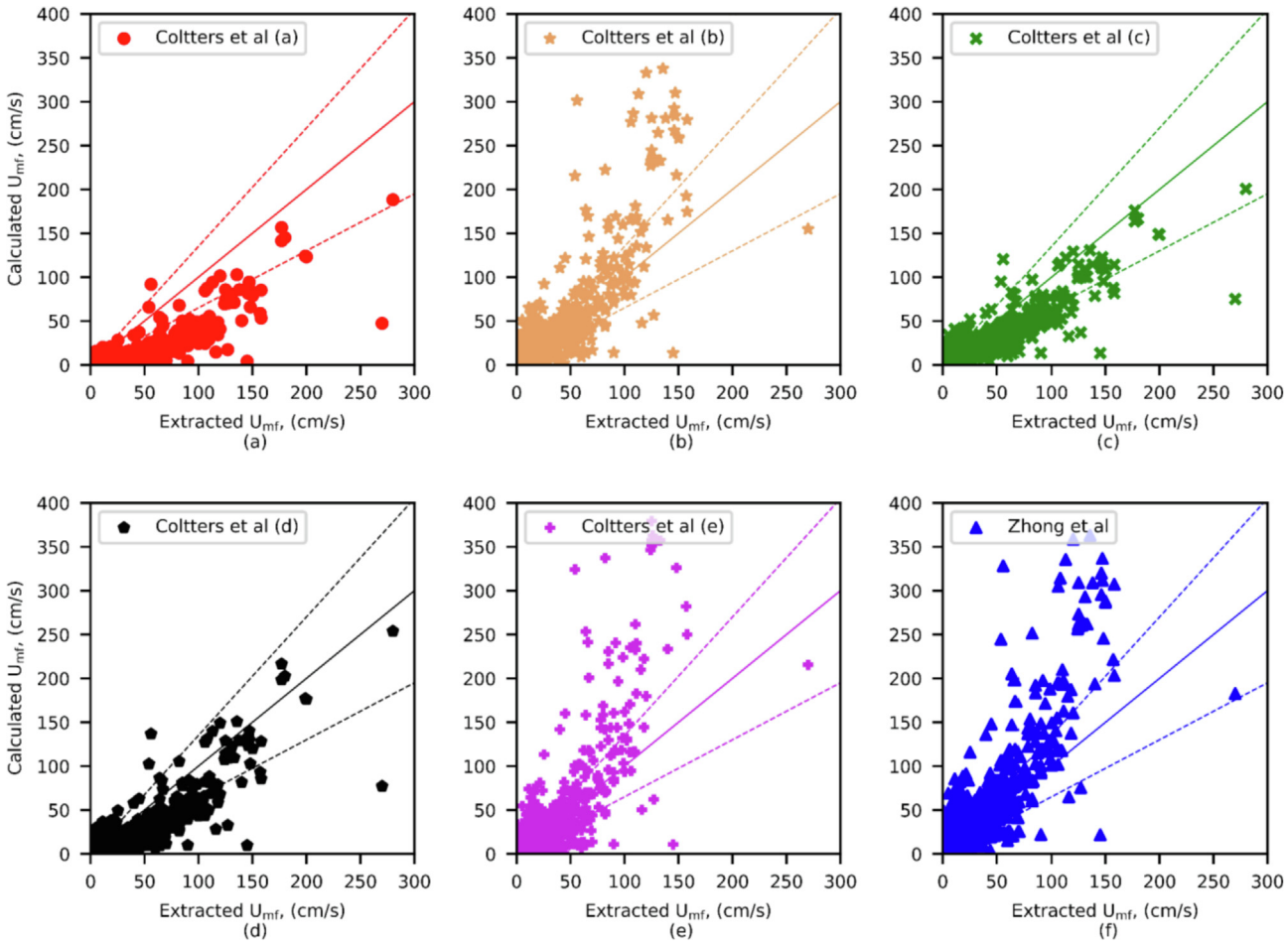

Fig. 2. Comparisons between the values of calculated and extracted U_{mf} for different correlations with $U_{mf} = K \cdot X^{\alpha}$ type.

particles, indicating that this type of correlation is completely not suitable for predicting U_{mf} of Geldart Group A particles. For Geldart Group B particles, only correlations of Coltters et al (c) and (d) (Coltters and Rivas, 2004) have the positive values of R^2, but they are small, only 0.162 and 0.129. And the corresponding values of *PC* are only 30.8% and 45.5%, respectively. The values of R^2 of Coltters et al. (c) and (d) (Coltters and Rivas, 2004) are 0.409 and 0.366 for Geldart Group D particles, and the corresponding values of *PC* are 50.2% and 44.2%, respectively. These above results demonstrate that this type of correlation also has high limitations and is only applicable to a small amount of Geldart Groups B and D particles. Obviously, this type of correlation cannot also be used as the general correlation to simultaneously predict U_{mf} of Geldart Groups A, B and D particles

In summary, this type of correlation only preforms well in a specific system, and it is not advisable to extrapolate this type of correlation to predict U_{mf} over a wide range of systems.

3.1.3. Performances of empirical correlations with $\boldsymbol{Re_{mf} = \frac{Ar}{p+q\sqrt{Ar}}}$ type

In this type of correlation, Re_{mf} is a function of both Ar and $\sqrt{Ar}$. Four correlations, as listed in Table 3, are selected and evaluated, and the results are shown in Fig. 3 and Figs. S7-S9.

As shown in Fig. 3, different from the results of the above two types of correlations, this type of correlation gives rather accept-

Table 3
Statistical analysis results for different correlations with $Re_{mf} = \frac{Ar}{p+q\sqrt{Ar}}$ type.

Researchers	Correlations	A			B			D			All		
		AARE	R^2	PC	AARE	R^2	PC	AARE	R^2	PC	AARE	R^2	PC
Todes et al (Todes, 1958)	$Re_{mf} = \frac{Ar}{1400+5.2\sqrt{Ar}}$	0.338	0.381	64.6%	0.284	0.494	75.7%	0.220	0.736	85.7%	0.279	0.875	76.1%
Davtyan et al. (Davtyan et al., 1976)	$Re_{mf} = \frac{Ar}{1040+4.86\sqrt{Ar}}$	0.446	0.490	50.3%	0.382	0.579	65.6%	0.176	0.817	89.1%	0.348	0.908	68.3%
Fletcher et al. (a) (Fletcher et al., 1992)	$Re_{mf} = \frac{Ar}{790+7\sqrt{Ar}}$	0.680	0.520	32.3%	0.508	0.552	50.1%	0.252	0.560	83.4%	0.480	0.822	54.5%
Fletcher et al. (b) (Fletcher et al., 1992)	$Re_{mf} = \frac{Ar}{1400+5\sqrt{Ar}}$	0.338	0.384	64.1%	0.283	0.501	76.1%	0.208	0.761	87.2%	0.276	0.884	76.6%

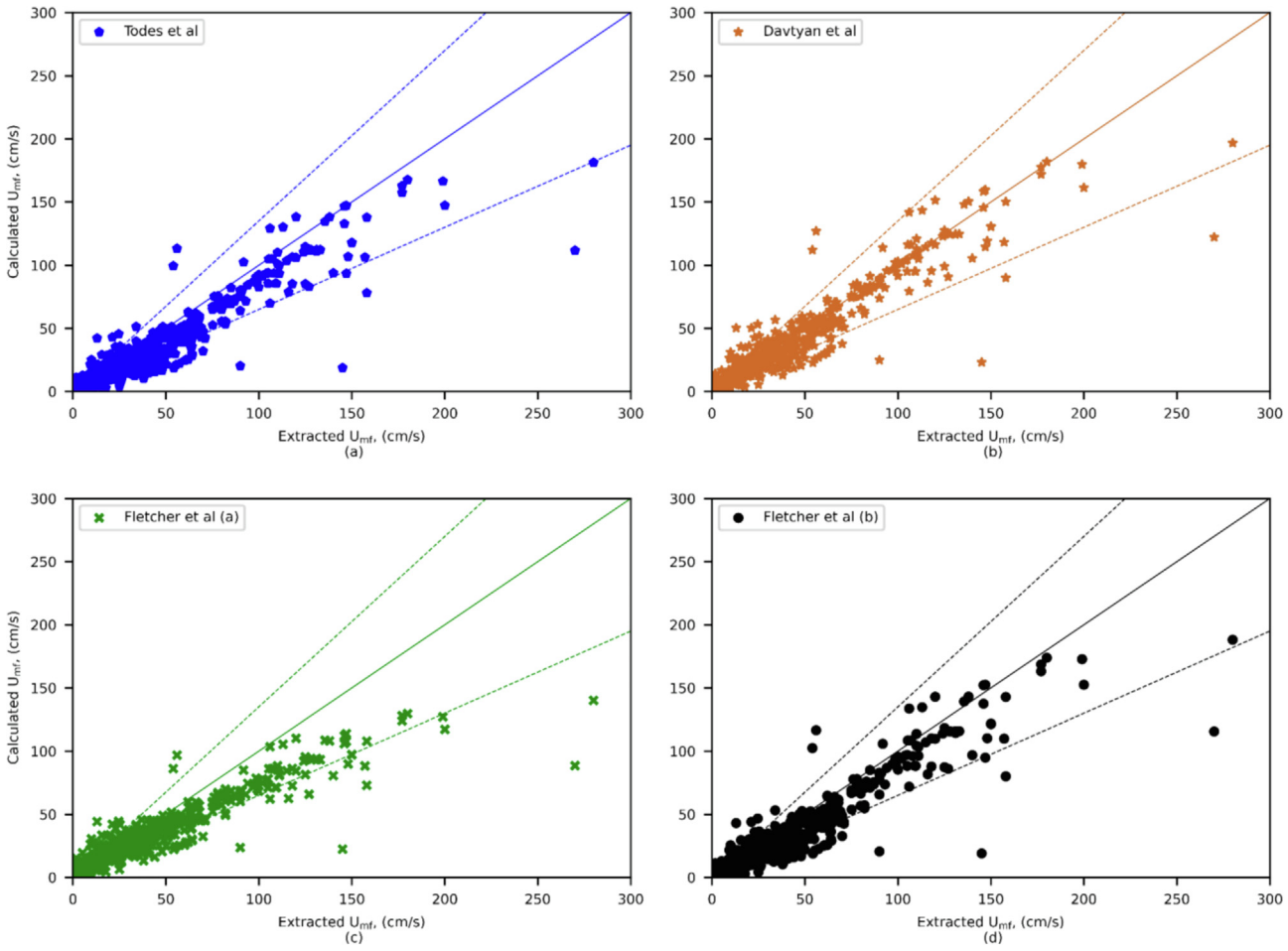

Fig. 3. Comparisons between the values of calculated and extracted U_{mf} for different correlations with $Re_{mf} = \frac{Ar}{p+q\sqrt{Ar}}$ type.

able predictive capability, and most of the data points are scattered within the relative error range. As depicted in Table 3, the values of R^2 of these four correlations are greater than 0.8, and the corresponding values of *PC* are all greater than 50%. Among them, the correlations of Todes et al. (1958) and Fletcher et al. (b) (Fletcher et al., 1992) give the better performances, and the corresponding values of *PC* are 76.1% and 76.6%, respectively. These results indicate that this type of correlation can be used as a general correlation to a certain extent with suitable empirical constants. In particular, as depicted in Fig. S9 and Table 3, for Geldart Group D particles, almost all of the data points are within the relative error range, the values of *PC* are 85.7%, 89.1%, 83.4%, and 87.2% and the corresponding values of R^2 are 0.736, 0.817, 0.560 and 0.761, respectively, indicating that this type of correlation can be confidently extrapolated to systems with almost all types of Geldart Group D particles. For Geldart Groups A and B particles, this type of correlation shows slightly lower predictive capability; the average values of *PC*, R^2, and *AARE* are 0.53, 0.44, 0.45 and 0.67, 0.53, 0.36, respectively. Besides, the correlation of Fletcher et al. (a) (Fletcher et al., 1992) yields the lowest predictive capability of each Geldart Group particle, which overestimates U_{mf} of Geldart Groups A and B particles (Figs. S7-S8) and underestimates U_{mf} of Geldart Group D particles (Fig. S9). The correlation of Fletcher et al. (b) (Fletcher et al., 1992) may be considered as the most suitable correlation among these four correlations for predicting U_{mf} of all Geldart Groups particles.

In summary, for this type of correlation, it is acceptable to predict U_{mf} of Geldart A, B and D particles at the same time with appropriate empirical parameters. Specially, it has been distinctly fitted with Geldart Group D particles, but it is slightly worse for Geldart Groups A and B particles, which is probably due to the lack of considering the inter-particle cohesive effect (Anantharaman et al., 2017).

3.1.4. Performances of empirical correlations with $Re_{mf} = (K_1^2 + K_2 Ar)^{0.5} - K_1$ type

To tackle the problem of lack of measured values for the bed voidage and particle sphericity, Wen et al. proposed a simplified form of Ergun equation by assigning values to the two lumped parameters (Wen and Yu, 1966):

$$\frac{1.75}{\varepsilon_{mf}^3 \varphi} = C_1 \tag{11}$$

$$\frac{150(1-\varepsilon_{mf})}{\varepsilon_{mf}^3 \varphi^2} = C_2 \tag{12}$$

$$C_1 Re_{mf}^2 + C_2 Re_{mf} = Ar \tag{13}$$

Eq. 13 can be rearranged into the form of Eq.14, and the relationship between Re_{mf} and Ar is given by introducing the parameters K_1 and K_2:

$$Re_{mf} = \left(K_1^2 + K_2 Ar\right)^{0.5} - K_1 \tag{14}$$

It is worth noting that this type of correlation is the most widely studied in the literature. And eight correlations listed in Table 4 are selected and evaluated. Fig. 4 and Figs. S10-S12 display the comparison results. Although this type of correlation generally gives acceptable predictive capability, correlations with different parameters still show significant discrepancies. As explicated in Table 4, ignoring the correlation of Babu et al. (1978), the values of R^2 range from 0.639 to 0.909, and the corresponding values of PC range from 53.6% to 77.0%. Moreover, in consistent with the previous results (Anantharaman et al., 2017), the correlation of Babu et al. (1978) obviously overestimates U_{mf}. Besides, the correlation of Hartman et al. (2000) underestimates U_{mf} for Geldart Group D particles but gives reasonable predictions for Geldart Groups A and B particles (Figs. S10-12). Except for the correlations of Babu et al. (1978) and Hartman et al. (2000), the average values of *PC* for Geldart Groups A, B, and D particles are 58.4%, 69.7%, and 87.8%, respectively, indicating that the applicability of these correlations to Geldart Groups B and D particles is better than that to Geldart Group A particles. This is similar to the results of the third type of correlation listed in Table 3.

In summary, this type of correlation generally provides acceptable predictive performances, especially for Geldart Groups B and D particles. Although the performance of this type of correlation for Geldart Group A particles is slightly worse, it is still better than the other three types of correlations.

Through the comprehensive evaluation of these four types of correlations with the extracted database, it is clearly understood that the predictive capabilities of these empirical correlations are quite different from each other. Although some of these correlations provide satisfactory performances, they exhibit remarkable differences in both general form and in sensitivity to empirical parameters. Herein, the third and fourth types of correlations exhibit the smallest discrepancy in U_{mf} predictions and provide the best overall coverage across all Geldart Groups particles, while the first and second types of correlations give the poor predictive capability and can only be applied to specific systems. This may be related to the location of the empirical parameters that need to be determined; for the first and second types, the parameters are in the exponential position, while the third and fourth types use fixed exponents (Anantharaman et al., 2017).

3.2. Performances of the modified correlations

In this section, we will firstly modify the above four types of correlations by determining the empirical parameters based on the extracted database. Then, we evaluate their performances in predicting U_{mf} of all Geldart Groups particles.

For the first type of correlation, $Re_{mf} = A \cdot Ar^b$ can be transformed to Eq.15 in the format of natural logarithm:

$$\log(Re_{mf}) = \log(A) + b \cdot \log(Ar) = K + \alpha \log(Ar) \tag{15}$$

where K and α are parameters that can be determined through regression analysis with the extracted database. Clearly, $\log(Re_{mf})$ and $\log(Ar)$ should have a linear relationship, which is confirmed in Fig. 5a by displaying the log–log plot of Re_{mf} against Ar. As shown in Fig. 5a, the equation excellently fits the data, and a closer scatter of the data points around this fitted line is seen with a correlation coefficient of R^2 = 0.961, then the slope and intercept of this line can be obtained:

$$\log(Re_{mf}) = -6.86853 + 0.90526 \log(Ar) \tag{16}$$

$$Re_{mf} = 0.001040 Ar^{0.905} \tag{17}$$

To assess this modified correlation, the values of the calculated and extracted U_{mf} are compared, and the results are shown in Fig. 6a, Fig. S13, and Table 5. As shown in Fig. 6a and Fig. S13, the trend of the curve is similar to that of Fig. 1, but the maximum discrepancy is substantially reduced. When predicting U_{mf} of all Geldart Groups particles, although the value of R^2 increases, it is still negative (-1.685), which is also caused by the huge error in

Table 4
Statistical analysis results for different correlations with $Re_{mf} = (K_1^2 + K_2 Ar)^{0.5} - K_1$ type.

Researchers	Correlations	A			B			D			All		
		AARE	R^2	PC	AARE	R^2	PC	AARE	R^2	PC	AARE	R^2	PC
Wen-Yu (Wen and Yu, 1966)	$Re_{mf} = (33.7^2 + 0.0408Ar)^{0.5} - 33.7$	0.357	0.382	56.9%	0.280	0.542	74.9%	0.175	0.813	88.7%	0.269	0.904	75.0%
Bourgeis et al. (Bourgeois and Grenier, 1968)	$Re_{mf} = (25.46^2 + 0.0382Ar)^{0.5} - 25.46$	0.343	0.469	66.2%	0.326	0.592	74.9%	0.186	0.817	89.1%	0.298	0.909	76.6%
Babu et al. (Babu et al., 1978)	$Re_{mf} = (25.25^2 + 0.0651Ar)^{0.5} - 25.25$	0.762	0.646	28.2%	0.933	0.097	18.8%	0.522	0.369	41.5%	0.816	0.725	25.2%
Biń (Biń, 1994)	$Re_{mf} = (27.31^2 + 0.0386Ar)^{0.5} - 27.31$	0.335	0.445	64.1%	0.301	0.585	76.1%	0.181	0.817	89.1%	0.281	0.908	77.0%
Hartman et al. (Hartman et al., 2000)	$Re_{mf} = (7.03^2 + 0.0101Ar)^{0.5} - 7.03$	0.340	0.404	64.6%	0.294	0.471	75.1%	0.393	0.025	32.8%	0.323	0.639	64.2%
Hilal et al. (Hilal et al., 2001)	$Re_{mf} = (13.07^2 + 0.0263Ar)^{0.5} - 13.07$	0.496	0.562	42.1%	0.524	0.549	45.0%	0.211	0.734	86.8%	0.451	0.879	53.6%
Mohanta et al. (Mohanta et al., 2012)	$Re_{mf} = (41.96^2 + 0.049Ar)^{0.5} - 41.96$	0.371	0.370	54.9%	0.284	0.535	73.7%	0.190	0.812	88.3%	0.277	0.903	73.8%
Tannous et al. (Tannous and Lourenço, 2015)	$Re_{mf} = (33.9^2 + 0.051Ar)^{0.5} - 33.9$	0.344	0.476	66.2%	0.335	0.597	73.8%	0.236	0.786	84.5%	0.315	0.899	74.9%

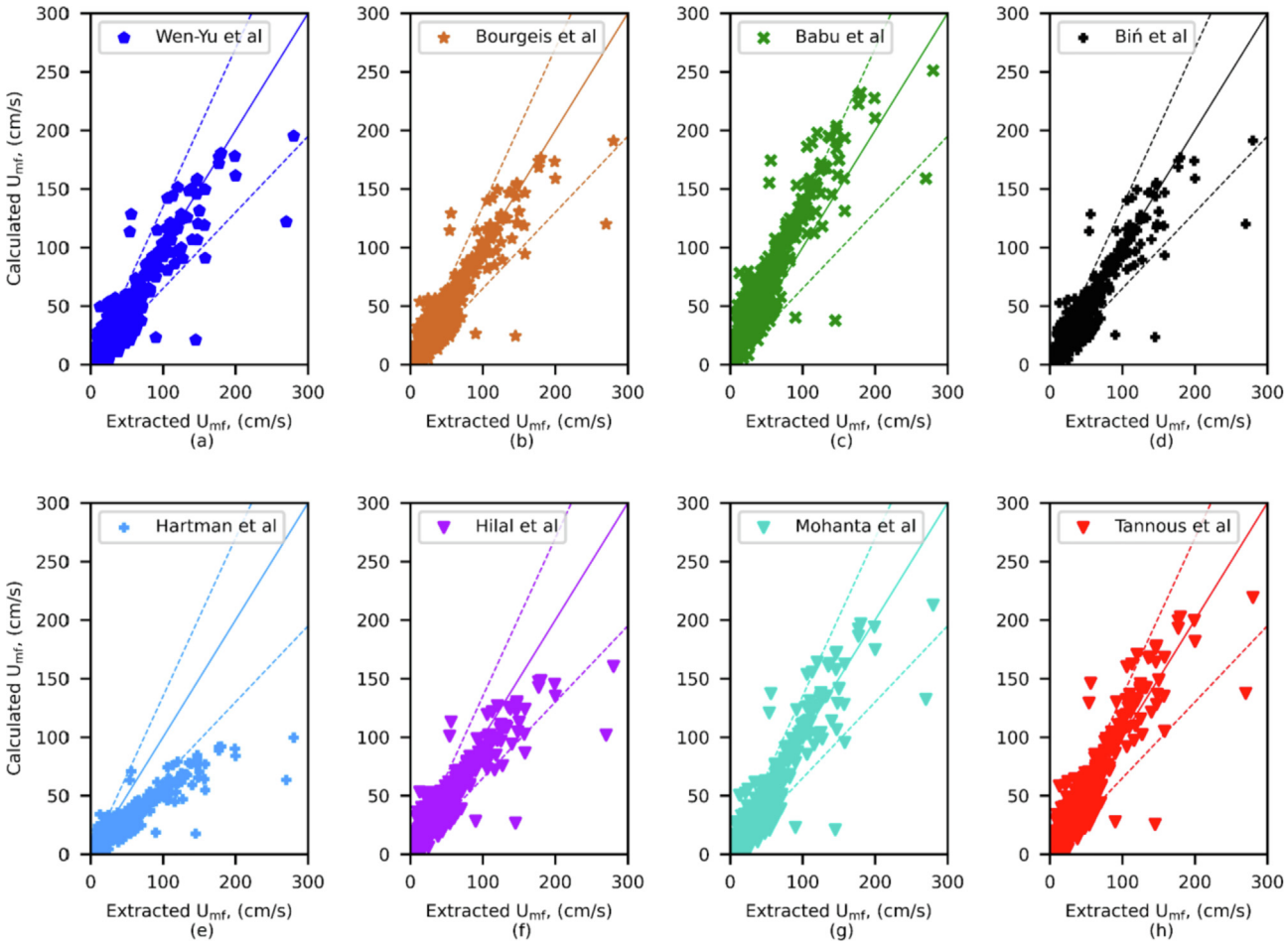

Fig. 4. Comparisons between the values of calculated and extracted U_{mf} for different correlations with $Re_{mf} = (K_1^2 + K_2 Ar)^{0.5} - K_1$ type.

predicting U_{mf} of Geldart Group D particles. For Geldart Groups A and B particles, compared with the best correlations of Fletcher et al. (1992) and Baeyens et al. (Baeyens and Geldart, 1973) listed in Table 1, this modified correlation shows the worse predictive capability with a lower R^2, a higher *AARE* and an almost identical *PC*. This unsatisfactory result may be related to the distribution of different Geldart Group particles in the extracted database. In this database, there are only 195 groups of Geldart Group A particles, and its proportion is 16.0%. While, the number of Geldart Groups B and D particles are 756 and 265, accounting for 62.2% and 21.8%, respectively. Therefore, the influence of Geldart Groups B and D particles in determining the parameters is greater than that of Geldart Group A particles. However, there is no doubt that this result once again testifies that this type of correlation is not suitable as a general correlation for simultaneously predicting U_{mf} of Geldart Groups A, B and D particle.

For the second type of correlation, a new equation in natural logarithmic form can also be obtained by converting Eq. 9 to Eq. 18:

$$\log(U_{mf}) = \log(\mathrm{K}) + \alpha \cdot \log(\mathrm{X}) \tag{18}$$

Similarly, a log–log plot of U_{mf} against X is plotted in Fig. 5b, and a line is also obtained by fitting the data. However, compared with Fig. 5a, a relative remoter scatter of the data points around the line is obtained with a lower correlation coefficient of R^2 = 0.769. Then the parameters (K and α) can be derived:

$$\log(U_{mf}) = -10.4713 + 0.6667\log(\mathrm{X}) \tag{19}$$

$$U_{mf} = 2.8338 * 10^{-5} X^{0.6667} \tag{20}$$

The evaluation results of this modified correlation are shown in Fig. 6b, Fig. S14, and Table 5. This modified correlation has a slightly better performance than the best correlation of Coltters et al. (d) (Coltters and Rivas, 2004) listed in Table 2. And the value of *AARE* decreases from 0.800 to 0.745, and the corresponding values of R^2 and *PC* increase from 0.725 to 0.730 and 40.7% to 44.2%, respectively. Concretely, for Geldart Groups A, B and D particles, the values of *AARE* decrease from 1.727 to 1.443, 0.700 to 0.694 and 0.406 to 0.376, the values of *PC* increase from 17.4% to 25.6%, 45.5% to 47.1% and 44.2% to 49.4%, but the values of R^2 decrease slightly. However, the negative value of R^2 of Geldart Group A particles and the lower values (much less than 1) of R^2 of Geldart Groups B and D particles testify that this modified correlation still cannot be confidently extrapolated to a wide range of systems.

For the third type of correlation, regression analysis can be performed after several steps of transformation. After the first transformation, Eq.21 can be obtained:

$$\frac{1}{Re_{mf}} = \frac{a + b\sqrt{Ar}}{Ar} = \frac{a}{Ar} + \frac{b}{\sqrt{Ar}} \tag{21}$$

then let $Re_{mf}^{'} = \frac{1}{Re_{mf}}, Ar^{'} = \frac{1}{\sqrt{Ar}}$, Eq.21 can be further simplified to Eq. 22:

$$Re_{mf}^{'} = \mathrm{b}Ar^{'} + \mathrm{a}Ar^{'2} \tag{22}$$

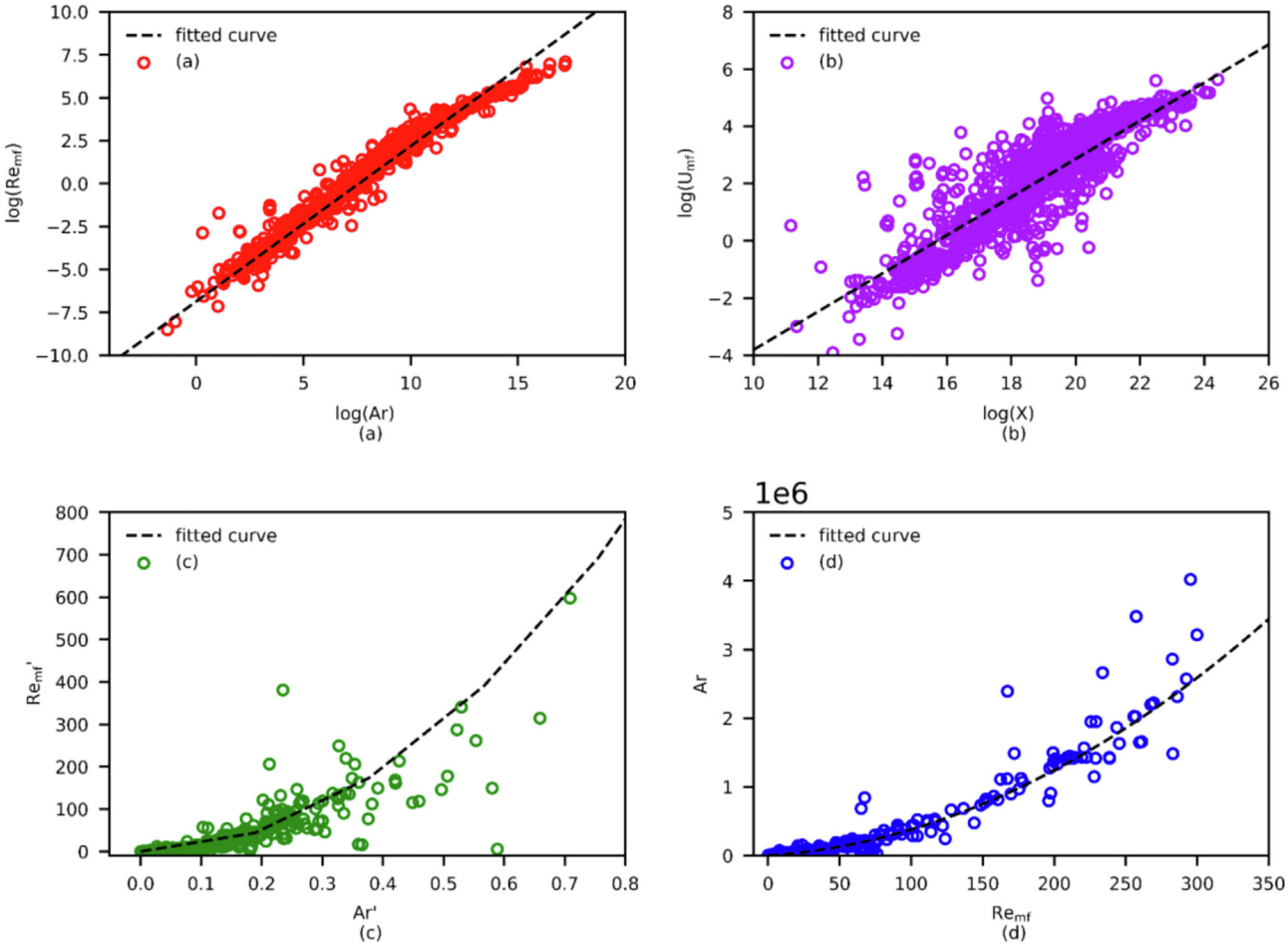

Fig. 5. Plots of log(Re_{mf}) versus log(Ar) (a), log(U_{mf}) versus log(Ar) (b), Re'_{mf} versus Ar' (c) and Ar versus Re_{mf} (d) with the extracted database.

Hence, the plot of Re'_{mf} against Ar' should yield a quadric curve, and this is verified in Fig. 5c. The correlation coefficient R^2, the first-order and the second order coefficients of the curve are then determined to be 0.903, 4.64 and 1208, respectively. Finally, this modified correlation is obtained:

$$Re_{mf} = \frac{Ar}{1208 + 4.64\sqrt{Ar}} \tag{23}$$

The evaluation results of this modified correlation are shown in Fig. 6c, Fig. S15, and Table 5. Compared with performances of the four correlations listed in Table 3, the predictive capability of this modified correlation in predicting U_{mf} of all Geldart Groups particles is slightly increased, with higher values of *PC* (76.4%) and R^2 (0.906), and a lower value of *AARE* (0.291). Concretely, for Geldart Group D particles, the values of *PC*, *AARE* and R^2 are 89.4%, 0.177 and 0.815, respectively, which are the same as the results of the correlation of Davtyan et al. (1976). While the values of *PC* of Geldart Groups A and B particles increase from 50.3% to 64.6% and 65.6% to 74.9%, and the values of *AARE* decrease from 0.446 to 0.368 and 0.382 to 0.311, respectively. This result indicates that this modified correlation can effectively improve the predictive capability of Geldart Groups A and B particles on the premise of ensuring the highly accurate prediction of Geldart Group D particles.

Lastly, the parameters in the fourth type of correlation are determined from Fig. 5d by plotting Re_{mf} against Ar with a correlation coefficient of R^2 = 0.792. It can be clearly seen that this fit is reasonable up to Re_{mf} of 300 and Ar up to 5.0×10^6. The modified correlation is shown in Eqs. 24–25:

$$24.275Re_{mf}^2 + 1354.354Re_{mf} = Ar \tag{24}$$

$$Re_{mf} = \left(27.896^2 + 0.0412Ar\right)^{0.5} - 27.896 \tag{25}$$

The evaluation results of this modified correlation are shown in Fig. 6d, Fig. S16, and Table 5. Regardless of the predictive capability of each Geldart Group particles or of all the Geldart Group particles, this modified correlation has almost the same performance as the correlation of Bourgeis et al. (Bourgeois and Grenier, 1968) Actually, this result is relatively easy to understand, considering that the wide distribution of particle diameter (86–25,000 μm) and particle density (1200–19,300 kg/m^3) investigated in their study (Bourgeois and Grenier, 1968), and their experimental conditions basically covered the database that we extracted.

In summary, with the extracted database, we proposed four modified correlations for different formulae. Compared with the published correlations, these modified correlations also have their limitations. But, on the whole, the third and fourth modified correlations can achieve satisfactory performances in predicting U_{mf} of all Geldart Groups particles, especially for Geldart Groups B and D particles.

Note that U_{mf} is essentially determined by the balance between the gravitational force and drag force of the gas-solid system, a new formula for U_{mf} prediction based on a fluidized bed drag cor-

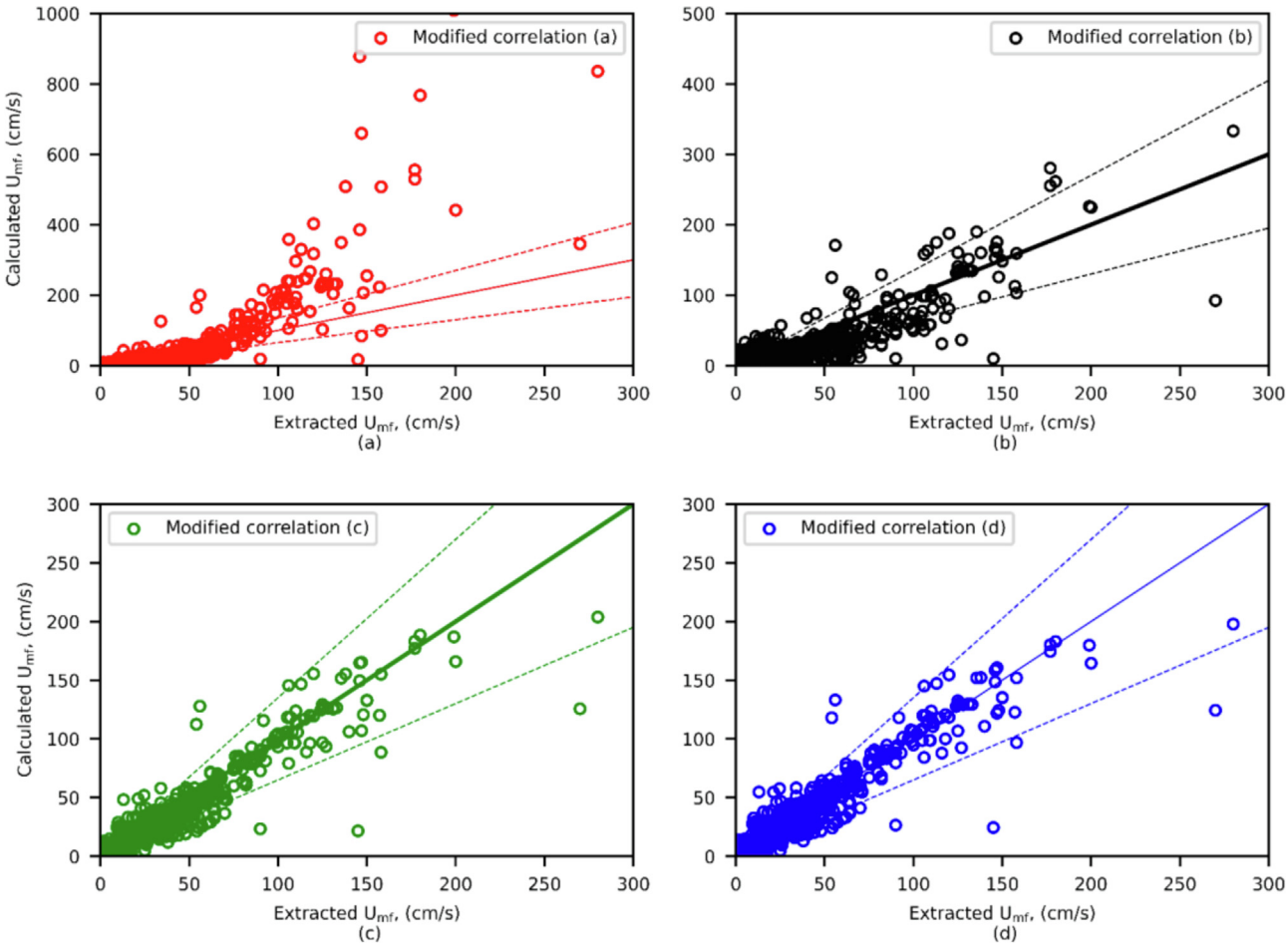

Fig. 6. Comparisons between the values of calculated U_{mf} and extracted U_{mf} with modified correlations.

Table 5
Statistical analysis result for different modified correlations.

Modified correlations	A			B			D			All		
	AARE	R^2	PC	AARE	R^2	PC	AARE	R^2	PC	AARE	R^2	PC
$Re_{mf} = 0.001040Ar^{0.905}$	0.358	0.304	65.1%	0.327	0.387	67.6%	0.534	−7.007	53.6%	0.377	−1.685	64.1%
$U_{mf} = 2.8338*10^{-5}X^{0.6667}$	1.443	−0.395	25.6%	0.694	0.112	47.1%	0.376	0.385	49.4%	0.745	0.730	44.2%
$Re_{mf} = \frac{Ar}{1208+4.64\sqrt{Ar}}$	0.368	0.443	64.6%	0.311	0.561	74.9%	0.177	0.815	89.4%	0.291	0.906	76.4%
$Re_{mf} = (27.896^2 + 0.0412Ar)^{0.5} - 27.896$	0.340	0.464	66.2%	0.320	0.593	75.3%	0.192	0.821	88.3%	0.296	0.910	76.6%
$1305.556Re_{mf} + 30.789Re_{mf}^{1.657} + 19.474Re_{mf}^2 = Ar$	0.348	0.465	66.7%	0.323	0.588	75.0%	0.186	0.824	88.7%	0.297	0.912	76.7%

relation derived from DNS is proposed. At the point of minimum fluidization, for a single isolated particle, gravity force (F_g) is balanced by the sum of buoyancy force (F_b) and drag force (F_d):

$$F_d = F_g - F_b = \frac{\pi d_p^3}{6}\left(\rho_s - \rho_g\right)g \tag{26}$$

Considering that F_g and F_b are only related to properties of particles and fluidized gases, thus, U_{mf} mainly depends on F_d. A variety of drag correlations have been proposed, and in this work, we selected the drag correlation proposed by Tang et al. (2015). In this correlation, the effect of particle mobility on the gas-solid drag force for dynamic gas-solid fluidized beds is considered. To be specific, the dimensionless drag force, defining by normalizing the drag force with Stokes drag force, can be expressed as the function of Re and solid volume fraction ($\varnothing$), shown in Eq.27:

$$F_d(\varnothing, Re) = \frac{10\varnothing}{(1-\varnothing)^2} + (1-\varnothing)^2\left(1 + 1.5\sqrt{\varnothing}\right) + \left[0.11\varnothing(1+\varnothing) - \frac{0.00456}{(1-\varnothing)^4} + \left(0.169(1-\varnothing) + \frac{0.0644}{(1-\varnothing)^4}\right)Re^{-0.343}\right]Re \tag{27}$$

This equation requires the measurement of $\varnothing$, to deal with the lack of measured values for $\varnothing$, simplify, these terms containing $\varnothing$ can be lumped into constants A, B and C in Eq.28:

$$F_d(\varnothing, Re) = A + \left(B + CRe^{-0.343}\right)Re \tag{28}$$

Stokes drag force at minimum fluidization can be given by Eq.29:

$$F_{d,Stokes} = 3\pi\mu d_p U_{mf} \tag{29}$$

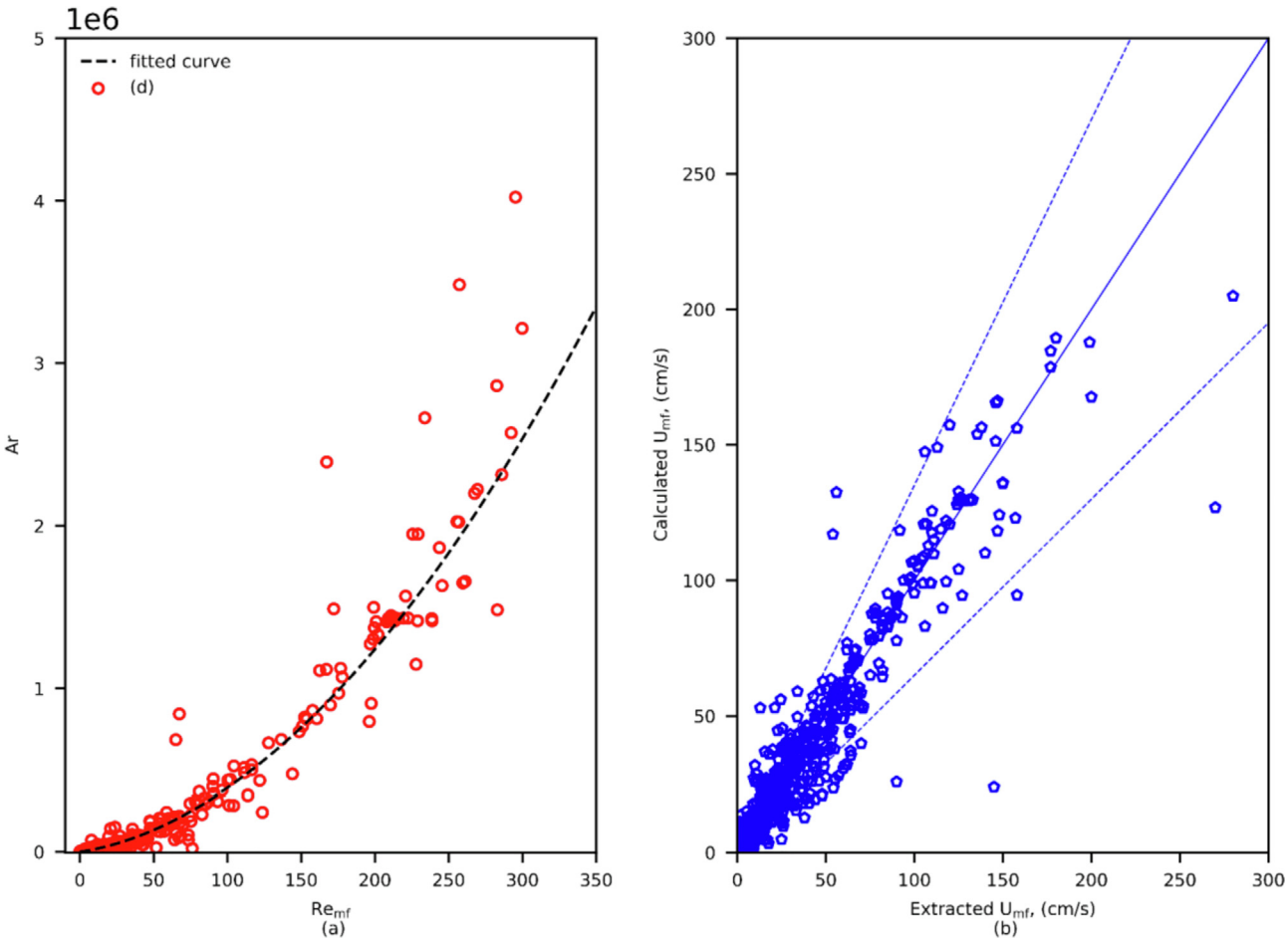

Fig. 7. Plot of Re_{mf} versus Ar_{mf} (a) and comparison between the values of calculated U_{mf} and the extracted U_{mf} with the new correlation (b).

Combining the Eqs.26, 28, and 29, the following equation can be obtained:

$$ARe_{mf} + BRe_{mf}^2 + CRe_{mf}^{1.657} = Ar \quad (30)$$

The right-hand side of this equation is Ar and the left-hand side is a function of Re_{mf}. Compared with the fourth type of correlation, Eq.30 has one more term and its exponent is 1.657. Then we obtain a plot of Re_{mf} against Ar shown in Fig. 7a, the parameters are also obtained through regression analysis, as shown in Eq.31:

$$1305.556Re_{mf} + 30.789Re_{mf}^{1.657} + 19.474Re_{mf}^2 = Ar \quad (31)$$

To test the validity of this new type of correlation, the values of calculated and extracted U_{mf} are compared and the results are given in Fig. 7b, Fig. S17, and Table 5. Compared with other four modified correlations and the published correlations, this new correlation gives the best performances with the highest values of R^2 and PC, and the almost identical value of $AARE$. This result indicates that this new formula of correlation can be used as a general correlation for the prediction of U_{mf} of all Geldart Groups particles in gas-solid fluidized beds and provides reasonable results for Re_{mf} values of up to 350 and Ar values of up to 5.0×10^6.

4. Conclusions

In this work, we use a recently established database of U_{mf} mined from published papers to assess the empirical correlations with four different formulae for Geldart Groups A, B, and D particles, respectively. Evaluation results show that the performances of correlations depend on the formulae and empirical parameters. Basically the correlations with formulae in which the parameters appear essentially in the exponential terms exhibit worse predictive ability. Furthermore, the discrepancies between the calculated and extracted U_{mf} for Geldart Group A particles are normally larger than that for Geldart Groups B and D particles. In view of that these empirical correlations have strong application limitations, modifications to different formulae have been made using the extracted database, to achieve satisfactory performances to predict U_{mf} for either Geldart Groups A, B, or D particles. A new type of correlation derived from a DNS based drag force model is also proposed. By use of this new formula, a general correlation is developed and the evaluation results show that it can predict the U_{mf} for Geldart Groups A, B, and D particles with performances superior over empirical correlations.

CRediT authorship contribution statement

Jibin Zhou: Conceptualization, Methodology, Writing – original draft. **Mao Ye:** Writing – review & editing, Supervision. **Zhongmin Liu:** Supervision.

Declaration of Competing Interest

The authors declare that they have no known competing financial interests or personal relationships that could have appeared to influence the work reported in this paper.

Acknowledgments

The authors thank the financial support from the National Natural Science Foundation of China (Grant No. 21991093 and 91834302) and the Natural Science Foundation of Liaoning province of China (2021-BS-011).

Appendix A. Supplementary material

Supplementary data to this article can be found online at https://doi.org/10.1016/j.ces.2022.117455.

References

Anantharaman, A., Cocco, R.A., Chew, J.W., 2017. Evaluation of correlations for minimum fluidization velocity (Umf) in gas-solid fluidization. Powder Technol. 323, 454–485.
Babu, S.P., Shah, P., Talwalker, A., 1978. Fluidization correlations for coal gasification materials-minimum fluidization velocity and fluidized bed expansion ratio. Chem. Eng. Prog. Symp. Ser. 1978 (74), 176–186.
Baeyens, J., Geldart, D., 1973. Predictive calculations of flow parameters in gas fluidised beds and fluidisation behaviour of various powders. In: Proceedings the International Symposium Fluidization and Its Applications. Cepadues Edition: Toulouse, France, pp. 263–273.
Bilbao, R., Lezaun, J., Abanades, J.C., 1987. Fluidization velocities of sand/straw binary mixtures. Powder Technol. 52 (1), 1–6.
Bińi, A.K., 1994. Prediction of the minimum fluidization velocity. Powder Technol. 81 (2), 197–199.
Bourgeois, P., Grenier, P., 1968. The ratio of terminal velocity to minimum fluidising velocity for spherical particles. Can. J. Chem. Eng. 46 (5), 325–328.
Chiba, S., Chiba, T., Nienow, A.W., Kobayashi, H., 1979. The minimum fluidisation velocity, bed expansion and pressure-drop profile of binary particle mixtures. Powder Technol. 22 (2), 255–269.
Coltters, R., Rivas, A.L., 2004. Minimum fluidation velocity correlations in particulate systems. Powder Technol. 147 (1-3), 34–48.
Davtyan, G.A., Ainshtein, V.G., Grigoryan, R.V., Amamchyeen, M.G., 1976. Izv. Akd. Nauk, Arm. SSR, Ser. Tekh. Nauk 26, 36.
Doichev, K., Akhmakov, N.S., 1979. Fluidisation of polydisperse systems. Chem. Eng. Sci. 34 (11), 1357–1359.
Fang, S., Wei, Y., Fu, L., Tian, G., Qu, H., 2020. Modeling of the minimum fluidization velocity and the incipient fluidization pressure drop in a conical fluidized bed with negative pressure. Appl. Sci. 10 (24), 8764. https://doi.org/10.3390/app10248764.
Feng, R., Li, J., Cheng, Z., Yang, X., Fang, Y., 2017. Influence of particle size distribution on minimum fluidization velocity and bed expansion at elevated pressure. Powder Technol. 320, 27–36.
Fletcher, J.V., Deo, M.D., Hanson, F.V., 1992. Re-examination of minimum fluidization velocity correlations applied to Group B sands and coked sands. Powder Technol. 69 (2), 147–155.
Geldart, D., 1973. Types of gas fluidization. Powder Technol. 7 (5), 285–292.
Gupta, S.K., Agarwal, V.K., Singh, S.N., Seshadri, V., Mills, D., Singh, J., Prakash, C., 2009. Prediction of minimum fluidization velocity for fine tailings materials. Powder Technol. 196 (3), 263–271.
Gutfinger, C., Abuaf, N., 1974. Heat transfer in fluidized beds. In: Advances in Heat Transfer. Elsevier, pp. 167–218.
Halvorsen, B.M., Arvoh, B., 2009. Minimum fluidization velocity, bubblebehaviour and pressure drop in fluidized beds with a range of particle sizes. WIT Trans. Eng. Sci., 227–238
Hartman, M., Trnka, O., Svoboda, K., 2000. Fluidization characteristics of dolomite and calcined dolomite particles. Chem. Eng. Sci. 55 (24), 6269–6274.
Hilal, N., Ghannam, M., Anabtawi, M., 2001. Effect of bed diameter, distributor and inserts on minimum fluidization velocity. Chem. Eng. Technol. 24, 161–165.
Hosseini, S.H., Karami, M., Altzibar, H., Olazar, M., 2019. Prediction of pressure drop and minimum spouting velocity in draft tube conical spouted beds using genetic programming approach. Can. J. Chem. Eng. 98, 583–589.
Jing, S., Hu, Q., Cai, G., Wang, J., Jin, Y., 2001. Introduction of particle plug valve. Powder Technol. 115 (1), 8–12.
Laugwitz, A., Rößger, P., Schurz, M., Richter, A., Meyer, B., 2017. Towards a validated CFD setup for a range of fluidized beds. Powder Technol. 318, 558–568.
Leva, M., 1959. Fluidization. McGraw-Hill Book Co. Inc, New York, NY.
Liu, Q., Shi, Y., Zhong, W., Yu, A., 2019. Co-firing of coal and biomass in oxy-fuel fluidized bed for CO_2 capture: a review of recent advances. Chin. J. Chem. Eng. 27 (10), 2261–2272.
Mahmoudi, S., Baeyens, J., Seville, J.P.K., 2010. NOx formation and selective non-catalytic reduction (SNCR) in a fluidized bed combustor of biomass. Biomass Bioenergy 34 (9), 1393–1409.
Mohanta, S., Daram, A.B., Chakraborty, S., Meikap, B.C., 2012. Characteristics of minimum fluidization velocity for magnetite powder used in an air dense medium fluidized bed for coal beneficiation. Part. Part. Syst. Char. 29 (4), 228–237.
Parise, M.R., Taranto, O.P., Kurka, P.R.G., Benetti, L.B., 2008. Detection of the minimum gas velocity region using Gaussian spectral pressure distribution in a gas–solid fluidized bed. Powder Technol. 182 (3), 453–458.
Pillai, B., Rao, M.R., 1971. Pressure drop and minimum fluidization velocities in air-fluidized beds. Indian J. Technol. 9, 77.
Sadeghbeigi, R., 2012. Fluid Catalytic Cracking Handbook: An Expert Guide to the Practical Operation, Design, and Optimization of FCC Units, third ed. Elsevier Science.
Sangeetha, V., Swathy, R., Narayanamurthy, N., Lakshmanan, C.M., Miranda, L.R., 2000. Minimum fluidization velocity at high temperatures based on geldart powder classification. Chem. Eng. Technol. 23 (8), 713–719.
Shao, Y., Li, Z., Zhong, W., Bian, Z., Yu, A., 2020. Minimum fluidization velocity of particles with different size distributions at elevated pressures and temperatures. Chem. Eng. Sci. 216, 115555. https://doi.org/10.1016/j.ces.2020.115555.
Subramani, H.J., Mothivel Balaiyya, M.B., Miranda, L.R., 2007. Minimum fluidization velocity at elevated temperatures for Geldart's group-B powders. Exp. Therm Fluid Sci. 32 (1), 166–173.
Tan, K.-K., Tan, Y.-W., Tey, B.-T., Look, K.-Y., 2008. On the onset of incipient fluidization. Powder Technol. 187 (2), 175–180.
Tang, Y., Peters, E.A.J.F., Kuipers, J.A.M., Kriebitzsch, S.H.L., Hoef, M.A.V.D., 2015. A new drag correlation from fully resolved simulations of flow past monodisperse static arrays of spheres. AIChE J. 61, 1958–1969.
Tannous, K., Lourenço, J.B., 2015. Fluid dynamic and mixing characteristics of biomass particles in fluidized beds. In: Innovative solutions in fluid-particle systems and renewable energy management. IGI Global, pp. 54–91.
Tian, P., Wei, Y., Ye, M., Liu, Z., 2015. Methanol to olefins (MTO): from fundamentals to commercialization. ACS Catal. 5 (3), 1922–1938.
Todes, O.M., Goroshkov, V.D., Rozenbaum, R.B., Izv. Vyssh. Uchcbn. Zaved. Neft Gaz, 1,1958.
Wang, J., Sun, Z., Shao, Y., Zhu, J., 2021. Operating regimes in circulating fluidized bed combustors: fast fluidization or bubbling-entrained bed? Fuel 297, 120727. https://doi.org/10.1016/j.fuel.2021.120727.
Wang, C., Zhu, J., 2020. Circulating fluidized beds, Essentials of Fluidization. In: Grace, J., Bi, X., Ellis, N. (Eds.), Essentials of Fluidization Technology. Wiley, pp. 239–268. https://doi.org/10.1002/9783527699483.ch12.
Wen, C.Y., Yu, Y.H., 1966. A generalized method for predicting the minimum fluidization velocity. AIChE J. 12 (3), 610–612.
Xu, C.C., Zhu, J., 2008. Prediction of the minimum fluidization velocity for fine particles of various degrees of cohesiveness. Chem. Eng. Commun. 196 (4), 499–517.
Zhong, W., Jin, B., Zhang, Y., Wang, X., Xiao, R., 2008. Fluidization of biomass particles in a gas-solid fluidized bed. Energy Fuels 22 (6), 4170–4176.
Zhou, J., Liu, D., Ye, M., Liu, Z., 2021. Data-Driven prediction of minimum fluidization velocity in gas-fluidized beds using data extracted by text mining. Ind. Eng. Chem. Res. 60 (37), 13727–13739.